

Securing Fresh Data in Wireless Monitoring Networks: Age-of-Information Sensitive Coverage Perspective

Jinwoong Kim, Minsu Kim, and Jemin Lee, *Member, IEEE*

Abstract—With the development of IoT, the sensor usage has been elevated to a new level, and it becomes more crucial to maintain reliable sensor networks. In this paper, we provide how to efficiently and reliably manage the sensor monitoring system for securing fresh data at the data center (DC). A sensor transmits its sensing information regularly to the DC, and the freshness of the information at the DC is characterized by the age of information (AoI) that quantifies the timeliness of information. By considering the effect of the AoI and the spatial distance from the sensor on the information error at the DC, we newly define an error-tolerable sensing (ETS) coverage as the area that the estimated information is with smaller error than the target value. We then derive the average AoI and the AoI violation probability of the sensor monitoring system, and finally present the η -coverage probability, which is the probability that the ETS coverage is greater than η ratio of the maximum sensor coverage. We also provide the optimal transmission power of the sensor, which minimizes the average energy consumption while guaranteeing certain level of the η -coverage probability. Numerical results validate the theoretical analysis and show the tendency of the optimal transmission power according to the maximum number of retransmissions. This paper can pave the way to efficient design of the AoI-sensitive sensor networks for IoT.

Index Terms—Age of information, sensor coverage, AoI violation probability, internet-of-things, monitoring networks

I. INTRODUCTION

The Internet of Things (IoT) and its enterprise-grade counterpart, the Industrial Internet of Things (IIoT) have been giving significant and positive influence to our lives and industries. With the development of the IoT technology, the sensor usage has been elevated to a new level. Sensors are devices that detect and respond to changes in an environment such as light, temperature, and motion. The reliable communication of the sensors becomes more crucial, especially for time-critical applications such as fault detection and emergency alarms. Therefore, to support the various applications of IoT, the maintaining reliable sensor network has been one of the challenges in IoT.

The design of reliable wireless sensor networks has been studied in many literature including the sensing coverage design [2]–[5]. The sensing coverage means the area that a

sensor can provide valid information from its measurement. The disk-based coverage model has been used as a simplest model in [2], and Elfes sensing model, which stochastically covers partial areas, was proposed in [3]. The sensing coverage was also determined by exploiting the spatial correlation of sensed information in [4], [5]. However, most of works in sensing coverage design did not consider the freshness of sensed information although the data freshness can affect the accuracy or the value of the information, especially in realtime applications such as health monitoring systems and road traffic reports [6].

The freshness of the data has been studied intensively after the concept of age of information (AoI) has been proposed. The AoI is a novel metric for measuring the data freshness, defined as the time elapsed since the generation of the most recently updated information [7]. In the early studies of the AoI, many works focused on the theoretical analysis of the AoI by considering the various queueing models [7]–[12]. For instance, the average AoI of M/M/1, M/D/1 and D/M/1 queues is investigated under the first-come-first-served (FCFS) policy in [7]. The average AoI of multi-source M/G/1 queue with the FCFS policy is derived in [8], while the average AoI and average peak AoI are analyzed with multi-server queueing model based on the last-come-first-served (LCFS) policy in [9] and with M/M/1/2* queue in [10]. The peak AoI outage probability has been presented for Geo/G/1 and D/G/1 queues, respectively, in [11], [12]. Furthermore, unlike the general AoI model in which the age increases linearly with time, a non-linear AoI model is also proposed in [13], [14] to represent the level of discontent for data staleness over time. Recently, as a variation of the AoI, the age of synchronization (AoS) is also presented in [15] to consider asynchronism issues between the AoI at the receiver and that at the source.

For communication reliability in AoI-based systems, the retransmission techniques have also been considered [16]–[19]. The average AoI is minimized by optimizing the redundancy allocation in the hybrid automatic repeat request (HARQ) scheme in [16]. In [17], the effect of the retransmission on AoI reduction is analyzed in the short packet-based machine type communications. In [18], the transmission power and the maximum allowable retransmission times are optimized to minimize the average AoI. However, as the feedback is not considered, the unnecessary transmissions can occur even after the successful update. The age-energy tradeoff is analyzed by comparing the retransmission and a transmission of newly generated update which pays for the sensing energy in [19].

J. Kim, M. Kim, and J. Lee are with the Department of Information and Communication Engineering, Daegu Gyeongbuk Institute of Science and Technology, Daegu 42988, South Korea (e-mail: yoy876@dgist.ac.kr, ads5577@dgist.ac.kr, jmnlee@dgist.ac.kr).

The material in this paper was presented, in part, at the Global Communications Conference, Taipei, Taiwan, Dec. 2020. [1]

The corresponding author is J. Lee.

Recently, for efficient design of AoI-based systems, the correlation among generated information at different sources has been exploited [20]–[22]. In [20], the average AoI was minimized by exploiting the temporal correlation between the consecutive updates. In [21], a correlated sensor apart from the exact source was exploited to decrease the sensing rate bearing a spatial error. The mutual information between the real-time source and received status updates are analyzed to quantify the freshness of information and optimized the sampling policy that maximizes the average mutual information in [22]. However, those works did not jointly consider the spatial and temporal correlation of sensing information, which fails to further enhance the sensing efficiency in the AoI-based system.

In this paper, we consider a sensor monitoring system, where a sensor periodically transmits the sensed regional information to a data center (DC) that requires maintaining fresh information, i.e., lower AoI. Within a sensing period, the retransmission scheme is also adopted with the limited maximum number of retransmissions. By exploiting the linear relationship between the AoI/the spatial distance from the sensor with the information error at the DC, we define the error-tolerable sensing (ETS) coverage, defined as the area that the estimated information at the DC is with smaller error than the target value. Under such circumstances, we characterize the components (e.g., time interval of successful updates at the DC) that affects the AoI, and derive the average AoI of the sensor monitoring system. After deriving the AoI violation probability, we also present the η -coverage probability, which is the probability that the ETS coverage is greater than η ratio of the maximum sensor coverage. Finally, we formulate the optimization problem for minimizing the average energy consumption of the sensor while guaranteeing certain level of η -coverage probability, and provide the optimal transmission power. The main contributions of this paper can be summarized as follows:

- we newly define the ETS coverage, which reflects the *spatial-temporal correlation* between the current exact information and the available information at the DC, which is a function of the AoI and the spatial distance from the sensing point;
- after deriving the AoI violation probability, we present a *closed-form expression of the η -coverage probability* and analytically show that the η -coverage probability increases with the transmission power of the sensor;
- from the trade-off between the transmission power and the average number of retransmissions, we formulate the average energy consumption minimization problem, and provide *the optimal transmission power of the sensor* for the noise-limited environments and the interference-limited environments; and
- we analytically show the optimal transmission power increases with the maximum number of retransmissions regardless of system parameters' values.

The remainder of this paper is organized as follows. In Section II, we present a network model, concept of the AoI and the η -coverage probability. In Section III, we derive the closed-form expression of the average AoI and the AoI violation

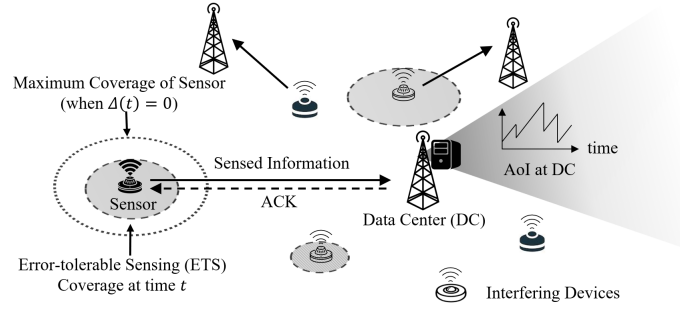


Fig. 1. An example of the sensor monitoring system.

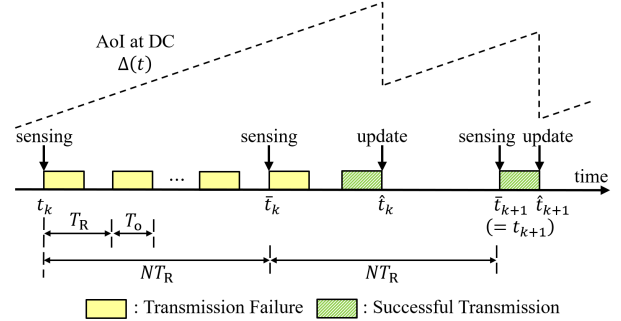


Fig. 2. Procedure of the retransmission at a sensor and the change of AoI at the DC.

probability. In Section IV, we formulate the average energy consumption minimization problem constrained on the target η -coverage probability. In Section V, we evaluate the theoretically obtained average AoI and AoI violation probability with the simulation and find the optimal transmission power to minimize the average energy consumption. Finally, the conclusion is presented in Section VI.

II. SYSTEM MODEL

In this section, we describe the network model and the AoI of the sensor monitoring system. We also present the sensing coverage model.

A. Network Model

We consider a sensor monitoring system, which consists of sensors and the DC, as shown in Fig. 1. Each sensor senses regional information (e.g., temperature, lighting, and humidity, etc.) periodically with the period T_s , and transmits it to the DC via wireless communications during given transmission duration T_o . The DC maintains the information of the sensor, and updates it whenever it successfully receives the sensed information from the sensor.

In this network, we assume there also exist IoT devices, which use the same frequency channel and interfere the communication of the sensor. Specifically, we assume there are J -types of interfering IoT devices with indices $\mathcal{J} = \{1, 2, \dots, J\}$, and the j -th type ($j \in \mathcal{J}$) interfering IoT devices are randomly distributed as a homogeneous Poisson point process (HPPP) Φ_j with the spatial density λ_j . When the transmission power

TABLE I
NOTATIONS USED THROUGHOUT THE PAPER.

Notation	Definition
p_s	Successful transmission probability
P_t	Transmission power of a sensor
P_j	Transmission power of j -th type interfering IoT device
h	Channel fading gain
d	Distance of the link between a sensor and DC
α	Pathloss exponent
N_o	Noise power
I	Interference at the DC
δ	Target SINR
λ_j	Density of j -th type interfering IoT devices
T_o	Transmission duration
T_R	Retransmission interval
N	Maximum number of retransmission
X_k	Time from the sensing instant after the $(k-1)$ th successful update to the k th successful update
Z_k	Time of the k th successful update from its sensing instant
Y_k	Waiting time for the next sensing after the k th successful update
Q_k	Trapezoid area between the $(k-1)$ th and the k th successful updates in AoI
U_k	Inter-arrival time between $(k-1)$ th and k th successful updates
t_k	Sensing time after the $(k-1)$ th successful update
\bar{t}_k	Sensing time of the k th successful update
\hat{t}_k	Time of the k th successful update
$\rho(r, t)$	Correlation of two information
$\epsilon(r, t)$	Estimation error
θ_{th}	Threshold of estimation error
$S_c(\theta_{th})$	Maximum sensing coverage of a sensor
$\mathcal{P}_c(\eta)$	η -coverage probability
$\bar{\Delta}$	Average AoI
$\mathcal{P}_v(v_{th})$	AoI violation probability
g_k	Violated time of the k th update
v_{th}	AoI violation threshold
$\mathcal{E}(P_t)$	Average energy consumption

of the sensor is P_t , the SINR received by the DC y_0 from the sensor x_0 can be expressed as

$$\text{SINR}_{x_0, y_0} = \frac{P_t h_{x_0, y_0} d_{x_0, y_0}^{-\alpha}}{I + N_o}, \quad (1)$$

where $h_{x,y}$ and $d_{x,y}$ are the channel fading gain and the distance of the link between nodes x and y , α is the pathloss exponent, and N_o is the the power of the additive white Gaussian noise (AWGN). Here, $I = \sum_{j \in \mathcal{J}} P_j \sum_{x \in \Phi_j} h_{x, y_0} d_{x, y_0}^{-\alpha}$ is the received interference power, where P_j is the transmission power of the j -type interfering IoT devices. We assume the channel experiences Rayleigh fading, i.e., $h_{x,y} \sim \exp(1) \forall x, y$.

The transmission of a sensor can be successfully received at the DC, when the SINR at the DC is greater than or

equal to the target SINR, δ . Then, the successful transmission probability (STP) can be presented as [23]¹

$$\begin{aligned} p_s &= \mathbb{P}[\text{SINR}_{x_0, y_0} \geq \delta] \\ &= \exp\left(-\frac{\xi}{P_t} - \frac{\zeta}{P_t^{2/\alpha}}\right) = f_s(P_t), \end{aligned} \quad (2)$$

where ζ and ξ are given by

$$\begin{aligned} \zeta &= \delta^{2/\alpha} d_{x_0, y_0}^2 C_1(\alpha) \sum_{j \in \mathcal{J}} \lambda_j P_j^{2/\alpha} \\ \xi &= N_o \delta d_{x_0, y_0}^\alpha \end{aligned}$$

for $C_1(\alpha) = \left(\frac{2\pi}{\alpha}\right) \Gamma\left(\frac{2}{\alpha}\right) \Gamma\left(1 - \frac{2}{\alpha}\right)$ with Gamma function $\Gamma(x) = \int_0^\infty t^{x-1} e^{-t} dt$. From (2), we can readily know that p_s can be presented as a function of P_t , i.e., $f_s(P_t)$, which increases with P_t .

Since the transmission from the sensor can be failed (with the probability $1 - p_s$), we consider the retransmission system, which allows the sensor to transmit up to N times, as shown in Fig 2. Specifically, the DC sends an ACK signal to the sensor once it successfully receives the information. If the sensor does not receive the ACK signal for certain amount of time, it retransmits until it receives the ACK signal or it senses new information. Hence, when the (re)transmission can be happened in every T_R (for $T_R > T_o$), the sensing period is the same as $T_s = NT_R$.

B. Age of Information

The DC updates the information of the sensor, when it receives the newly sensed information successfully. To measure the freshness of the sensor information at the DC at time t , we use the AoI, which is defined as [7]

$$\Delta(t) = t - t_o \quad (3)$$

where t_o is the sensing time of the most recently updated information at the DC. As shown in Fig. 3, we can see that the AoI increases linearly from the sensing instant over time, and then drops to the age of the updated information.

C. η -Coverage Probability

In the sensor monitoring networks, the sensed information is generally correlated in time and space [21]. For instance, the sensed information of a sensor at time t can have the correlation with that of the sensor at different location at a distance l and time $t + \tau$. We denote the correlation of those information as $\rho(l, \tau)$ for the distance difference l and the time difference τ between sensors, which can be presented using the covariance model as [21]

$$\rho(l, \tau) = \exp\{-ul - v\tau\} \quad (4)$$

for the scaling parameters u and v . When those information have correlation as (4), we can estimate the sensed information of a sensor at time $t + \tau$ from that of the other sensor at time t , and the estimation error can be presented as [21]

$$\epsilon(l, \tau) = 1 - \rho(l, \tau)^2 = 1 - \exp\{-2ul - 2v\tau\}. \quad (5)$$

¹This can be obtained by using the Laplace transform of interference and the cumulative distribution function (CDF) of the exponential distribution.

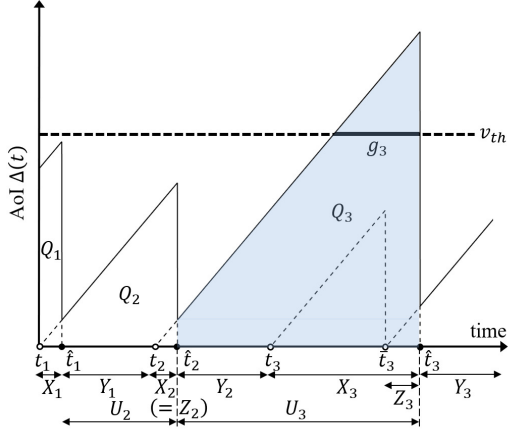


Fig. 3. An example of AoI path at a DC

We now define the error-tolerable sensing (ETS) coverage of a sensor. The ETS coverage is the area that the sensor can provide valid information with smaller error than θ_{th} at $t + \tau$ from its sensing information at t . From (5), the ETS coverage can be presented as a circle with the radius $r(\tau, \theta_{\text{th}})$, given by

$$\begin{aligned} \epsilon(l, \tau) &\leq \theta_{\text{th}} \\ \Leftrightarrow r(\tau, \theta_{\text{th}}) &\leq \frac{-\ln(1 - \theta_{\text{th}}) - 2v\tau}{2u}. \end{aligned} \quad (6)$$

From (6), we can see that $r(\tau, \theta_{\text{th}})$ is the maximum when $\tau = 0$ (i.e., at the sensing time), which is equal to $r_{\text{max}}(\theta_{\text{th}}) = \frac{-\ln(1 - \theta_{\text{th}})}{2u}$. Then, $r(\tau, \theta_{\text{th}})$ gets smaller over the time difference τ , as shown in Fig. 1. This means when the AoI of the sensor's information at the DC is $\Delta(t)$ at time t , the radius of the ETS coverage can be presented as

$$r(\Delta(t), \theta_{\text{th}}) = \sqrt{\frac{S_c(\theta_{\text{th}})}{\pi}} - \frac{v}{u}\Delta(t) \quad (7)$$

where $S_c(\theta_{\text{th}}) = \pi r_{\text{max}}^2(\theta_{\text{th}})$ is the maximum ETS coverage.

Using (7), we now define the η -coverage probability $\mathcal{P}_c(\eta)$ as the probability that the ETS coverage is more than η portion of the maximum ETS coverage $S_c(\theta_{\text{th}})$, given by

$$\mathcal{P}_c(\eta) = \mathbb{P}\left[\frac{\pi r^2(\Delta(t), \theta_{\text{th}})}{S_c(\theta_{\text{th}})} \geq \eta\right]. \quad (8)$$

Using (7) and (8), we can represent $\mathcal{P}_c(\eta)$ as

$$\begin{aligned} \mathcal{P}_c(\eta) &= \mathbb{P}\left[\Delta(t) \leq \frac{u}{v}\sqrt{\frac{S_c(\theta_{\text{th}})}{\pi}}(1 - \sqrt{\eta})\right] \\ &= 1 - \mathcal{P}_v\left(\frac{u}{v}\sqrt{\frac{S_c(\theta_{\text{th}})}{\pi}}(1 - \sqrt{\eta})\right) \end{aligned} \quad (9)$$

where $\mathcal{P}_v(v_{\text{th}}) = \mathbb{P}[\Delta(t) > v_{\text{th}}]$ is the AoI violation probability, which will be derived in the following section. This metric can show how large sensing area of the regional information the sensor has with smaller error than θ_{th} .

III. AGE OF INFORMATION ANALYSIS

In this section, we analyze the average AoI and the AoI violation probability of the sensor monitoring system. For the

analysis, we first define some notations, which is also used to present the AoI path at the DC in Fig. 3.

We denote t_k as the first sensing time after the $(k-1)$ th successful update, \bar{t}_k as the sensing time of the k th successful update, and \hat{t}_k as the time of the k th successful update at the DC. Note that t_k and \bar{t}_k can be either the same or different (e.g., $t_2 = \bar{t}_2$ in Fig. 3). After the $(k-1)$ th successful update, the interval from the first sensing time t_k to the k th successful update time \hat{t}_k is denoted as $X_k = \hat{t}_k - t_k$. Since X_k is determined by the number of retransmissions until the successful reception, its distribution can be modeled as the geometry distribution, of which the probability mass function (PMF) of X_k is given by

$$\mathbb{P}[X_k = (n-1)T_R + T_o] = (1 - p_s)^{n-1} p_s, \quad n = 1, 2, \dots \quad (10)$$

For the k th successful update, we denote the interval from its sensing time \bar{t}_k to the successful update time \hat{t}_k as $Z_k = \hat{t}_k - \bar{t}_k$. The distribution of Z_k also follows the geometric distribution, but it is truncated by the maximum number of the retransmission N as²

$$\mathbb{P}[Z_k = (n-1)T_R + T_o] = \frac{(1 - p_s)^{n-1} p_s}{1 - (1 - p_s)^N}, \quad n = 1, \dots, N. \quad (11)$$

After the k th successful update at \hat{t}_k , the time to the next sensing, i.e., t_{k+1} , is denoted as Y_k , given by

$$Y_k = t_{k+1} - \hat{t}_k = NT_R - Z_k. \quad (12)$$

We then denote the interval between the $(k-1)$ th and the k th successful updates at the DC as U_k , given by

$$U_k = \hat{t}_{k+1} - \hat{t}_k = Y_{k-1} + X_k. \quad (13)$$

A. Average AoI

We first analyze the average AoI of the system. The average AoI at the DC can be given by [8]

$$\begin{aligned} \bar{\Delta} &= \lim_{T \rightarrow \infty} \frac{1}{T} \int_0^T \Delta(t) dt \\ &= \lim_{T \rightarrow \infty} \left\{ \frac{Q_1 + Q_R}{T} + \frac{L(T) - 1}{T} \frac{1}{L(T) - 1} \sum_{k=2}^{L(T)} Q_k \right\} \\ &\approx \frac{\mathbb{E}[Q_k]}{\mathbb{E}[U_k]}, \end{aligned} \quad (14)$$

where Q_k is the trapezoid area between the $(k-1)$ th and the k th successful updates, $L(T) = \max\{k \mid \hat{t}_k \leq T\}$ is the number of the successful updates until time T and $Q_R = \frac{1}{2}(2Z_{L(T)} + T - \hat{t}_{L(T)})(T - \hat{t}_{L(T)})$ is the residual area after the last update to T . In the following Lemma, using (14), we obtain the average AoI.

Lemma 1: The average AoI of the sensor monitoring system can be expressed as

$$\bar{\Delta} = T_R \left\{ \frac{1}{p_s} + \frac{N-2}{2} \right\} + T_o. \quad (15)$$

²As Z_k is defined from the sensing time of the specific k th successful update, it cannot be greater than $(N-1)T_R + T_o$.

$$\mathcal{P}_v(v_{\text{th}}) = \begin{cases} \frac{\{p_s(T_o - T_R - v_{\text{th}}) + T_R\} \left\{1 - (1 - p_s)^{\lfloor \frac{v_{\text{th}} - T_o}{T_R} \rfloor + 1}\right\} + p_s T_R \left\{N - \left(\left\lfloor \frac{v_{\text{th}} - T_o}{T_R} \right\rfloor + 1\right)(1 - p_s)^{\lfloor \frac{v_{\text{th}} - T_o}{T_R} \rfloor + 1}\right\}}{p_s N T_R}, & \text{if } v_{\text{th}} \leq N T_R, \\ \frac{\{p_s T_R \lfloor \frac{v_{\text{th}} - T_o}{T_R} \rfloor + T_R + p_s T_o - p_s v_{\text{th}}\} \left\{(1 - p_s)^{\lfloor \frac{v_{\text{th}} - T_o}{T_R} \rfloor - N + 1} - (1 - p_s)^{\lfloor \frac{v_{\text{th}} - T_o}{T_R} \rfloor + 1}\right\}}{p_s N T_R}, & \text{if } v_{\text{th}} > N T_R. \end{cases} \quad (16)$$

Proof: From Fig. 3, the expectations of Q_k and U_k in (14) are, respectively, expressed as

$$\begin{aligned} \mathbb{E}[Q_k] &= \mathbb{E}\left[\frac{1}{2}(Y_{k-1} + X_k)(2Z_{k-1} + Y_{k-1} + X_k)\right] \\ &= \mathbb{E}\left[\frac{1}{2}(N T_R + X_k - Z_{k-1})(N T_R + X_k + Z_{k-1})\right] \\ &\stackrel{(a)}{=} \frac{1}{2}\mathbb{E}\left[(N T_R + X_k)^2\right] - \frac{1}{2}\mathbb{E}[Z_k^2], \end{aligned} \quad (17)$$

$$\begin{aligned} \mathbb{E}[U_k] &= \mathbb{E}[Y_{k-1} + X_k] = \mathbb{E}[N T_R - Z_{k-1} + X_k] \\ &\stackrel{(b)}{=} N T_R - \mathbb{E}[Z_k] + \mathbb{E}[X_k] \end{aligned} \quad (18)$$

where (a) and (b) follows since Z_{k-1} and Z_k are identically distributed. From (10), $\mathbb{E}[X_k]$ and $\mathbb{E}[X_k^2]$ are obtained, respectively, as

$$\begin{aligned} \mathbb{E}[X_k] &= \sum_{n=1}^{\infty} \{(n-1)T_R + T_o\} (1-p_s)^{n-1} p_s \\ &= \left(\frac{1}{p_s} - 1\right) T_R + T_o, \end{aligned} \quad (19)$$

$$\begin{aligned} \mathbb{E}[X_k^2] &= \sum_{n=1}^{\infty} \{(n-1)T_R + T_o\}^2 (1-p_s)^{n-1} p_s \\ &= \frac{2T_R^2}{p_s^2} - \frac{(3T_R - 2T_o)T_R}{p_s} + (T_R - T_o)^2. \end{aligned} \quad (20)$$

Similarly, from (11), we obtain $\mathbb{E}[Z_k]$ and $\mathbb{E}[Z_k^2]$, respectively, as

$$\begin{aligned} \mathbb{E}[Z_k] &= \sum_{n=1}^N \{(n-1)T_R + T_o\} \frac{(1-p_s)^{n-1} p_s}{1 - (1-p_s)^N} \\ &= \frac{T_R \left\{1 - (1-p_s)^N (1 + p_s N)\right\}}{p_s \left\{1 - (1-p_s)^N\right\}} - T_R + T_o, \end{aligned} \quad (21)$$

$$\begin{aligned} \mathbb{E}[Z_k^2] &= \sum_{n=1}^N \{(n-1)T_R + T_o\}^2 \frac{(1-p_s)^{n-1} p_s}{1 - (1-p_s)^N} \\ &\stackrel{(a)}{=} (T_R - T_o)^2 + \frac{T_R}{p_s \left\{1 - (1-p_s)^N\right\}} \left[\frac{T_R}{p_s} \left\{-N^2(1-p_s)^{N+2} \right. \right. \\ &\quad \left. \left. + (2N^2 + 2N - 1)(1-p_s)^{N+1} - (N+1)^2(1-p_s)^N - p_s \right. \right. \\ &\quad \left. \left. + 2\right\} - 2(T_R - T_o) \left\{1 - (1-p_s)^N (1 + p_s N)\right\} \right] \end{aligned} \quad (22)$$

where (a) is obtained from the equation in [24, eq. (0.114)]. By substituting (19), (20) and (22) into (17), and (19) and (21) into (18), $\mathbb{E}[Q_k]$ and $\mathbb{E}[U_k]$ are presented, respectively, as

$$\mathbb{E}[Q_k] = \frac{N T_R \left\{2 + (N-2)p_s T_R + 2p_s T_o\right\}}{2p_s \left\{1 - (1-p_s)^N\right\}}, \quad (23)$$

$$\mathbb{E}[U_k] = \frac{N T_R}{1 - (1-p_s)^N}. \quad (24)$$

Finally, substituting (23) and (24) into (14) results in (15). ■ From Theorem 1, we can see that the average AoI increases linearly with the retransmission duration T_R and the maximum number of the retransmissions N . In addition, we can also see that the average AoI decreases with p_s , since $\frac{d}{dp_s} \bar{\Delta} = -\frac{T_R}{p_s^2}$ is negative as T_R and p_s are positive.

B. AoI Violation Probability

In this subsection, we derive the closed-form expression of the AoI violation probability. The AoI violation probability can be defined as [25]

$$\mathcal{P}_v(v_{\text{th}}) = \mathbb{P}[\Delta(t) > v_{\text{th}}] = \lim_{T \rightarrow \infty} \frac{1}{T} \sum_{k=1}^{L(T)} g_k = \frac{\mathbb{E}[g_k]}{\mathbb{E}[U_k]}, \quad (25)$$

where g_k is the violated time duration of the k th successful update (as illustrated in Fig. 3).

Theorem 1: The AoI violation probability $\mathcal{P}_v(v_{\text{th}})$ of sensor monitoring system is given in (16), as shown at the top of this page, where $\lfloor \cdot \rfloor$ is a floor function.

Proof: See Appendix A. ■

From Theorem 1, we can express the η -coverage probability in (9) as the closed-form. In addition, we obtain the following corollary.

Corollary 1: The AoI violation probability decreases with the STP p_s , i.e., $\frac{d\mathcal{P}_v(v_{\text{th}})}{dp_s} \leq 0$.

Proof: Firstly, when $v_{\text{th}} \leq N T_R$, the derivative of $\mathcal{P}_v(v_{\text{th}})$ with respect to p_s is given by the first equation in (26), where $\beta_1 = T_R - p_s \alpha_1$ and $\alpha_1 = v_{\text{th}} - \left(\left\lfloor \frac{v_{\text{th}} - T_o}{T_R} \right\rfloor + 1\right) T_R$ with $0 \leq \alpha_1 \leq T_R$, then $(1-p_s)T_R \leq \beta_1 \leq T_R$. Here, we define the numerator of the first equation in (26) as $\bar{N}_{v,1}(p_s, \beta_1)$, which has the maximum value when $\beta_1 = T_R$. This is because

$$\frac{d\mathcal{P}_v(v_{\text{th}})}{dp_s} = \begin{cases} \frac{(1-p_s)^{\lfloor \frac{v_{\text{th}}-T_0}{T_R} \rfloor} \left\{ T_R(1-p_s) + \left(\lfloor \frac{v_{\text{th}}-T_0}{T_R} \rfloor + 1 \right) p_s \beta_1 - \left(\lfloor \frac{v_{\text{th}}-T_0}{T_R} \rfloor + 1 \right) p_s^2 (T_R - T_0) \right\} - T_R}{NT_R p_s^2}, & \text{if } v_{\text{th}} \leq NT_R, \\ \frac{(1-p_s) \left[(1-p_s)^{N-1} \left\{ T_R(1-p_s) + Np_s \beta_2 - Np_s^2 (T_R - T_0) \right\} - T_R \right] - \gamma p_s (\beta_2 + p_s T_0 - p_s T_R) \left\{ 1 - (1-p_s)^N \right\}}{NT_R p_s^2 (1-p_s)^{1-\gamma}}, & \text{if } v_{\text{th}} > NT_R. \end{cases} \quad (26)$$

$\bar{N}_{v,1}(p_s, \beta_1)$ increases with β_1 . We then obtain the derivative of $\bar{N}_{v,1}(p_s, T_R)$ with respect to p_s as

$$\frac{d}{dp_s} \bar{N}_{v,1}(p_s, T_R) = - \left(\lfloor \frac{v_{\text{th}} - T_0}{T_R} \rfloor + 1 \right) p_s (1-p_s)^{\lfloor \frac{v_{\text{th}} - T_0}{T_R} \rfloor - 1} \left\{ \lfloor \frac{v_{\text{th}} - T_0}{T_R} \rfloor T_0 + (T_R - T_0) \left(\lfloor \frac{v_{\text{th}} - T_0}{T_R} \rfloor + 2 \right) (1-p_s) \right\} \leq 0, \quad (27)$$

where $T_R - T_0 \geq 0$. From (27) and the fact that $\bar{N}_{v,1}(p_s, \beta_1)$ increases with β_1 , $\bar{N}_{v,1}(p_s, \beta_1)$ is not higher than $\bar{N}_{v,1}(p_s, T_R)$. Moreover, since $\bar{N}_{v,1}(0, \beta_1) = 0$, we can see that $\bar{N}_{v,1}(p_s, \beta_1)$ is negative. Therefore, $\mathcal{P}_v(v_{\text{th}})$ monotonically decreases with p_s . On the other hand, when $v_{\text{th}} > NT_R$, the derivative of $\mathcal{P}_v(v_{\text{th}})$ with respect to p_s is given by (26), where $\beta_2 = T_R(1 + Np_s) - p_s(v_{\text{th}} - \gamma T_R)$ with $\gamma = \lfloor \frac{v_{\text{th}} - T_0}{T_R} \rfloor - N + 1 \geq 1$, then $T_R \leq \beta_2 < T_R(1 + p)$. The numerator of the second equation in (26) has two parts: (a) and (b). The fact that (a) is negative can be proven in the same way as the first case (i.e., $v_{\text{th}} \leq NT_R$). In addition, (b) is negative due to $\beta_2 + p_s T_0 - p_s T_R > 0$. Therefore, $\mathcal{P}_v(v_{\text{th}})$ monotonically decreases with p_s . ■

From Corollary 1, it can be seen that the AoI violation probability decreases as the transmission power increases or the distance between the sensor and DC decreases.

IV. AVERAGE ENERGY CONSUMPTION MINIMIZATION

In this subsection, we consider the average energy consumption minimization problem of the sensor monitoring system. The average energy consumption of the system $\mathcal{E}(P_t)$ per retransmission interval T_R is given by

$$\mathcal{E}(P_t) = \frac{E_s + \bar{N} P_t T_0}{N}, \quad (28)$$

where E_s is the sensing energy and \bar{N} is the average number of retransmissions per the sensing period NT_R , which can be represented as

$$\begin{aligned} \bar{N} &= \sum_{n=1}^N n (1-p_s)^{n-1} p_s + N (1-p_s)^N \\ &= \frac{1 - (1-p_s)^N}{p_s}. \end{aligned} \quad (29)$$

Note that, in (28), there is a trade-off between the transmission energy $P_t T_0$ and the average number of retransmissions \bar{N} .

Specifically, as the transmission power P_t increases, $P_t T_0$ increases, but \bar{N} decreases because $\frac{d\bar{N}}{dp_s} < 0$ in (29). Therefore, we consider the problem of the average energy consumption minimization by optimizing P_t while guaranteeing the η -coverage probability not less than the target probability ϵ as follows.

Problem 1 (Average Energy Consumption Minimization Problem):

$$\begin{aligned} \min_{P_t} \quad & \frac{E_s}{N} + \frac{T_0 P_t \left\{ 1 - (1-p_s)^N \right\}}{N p_s} \\ \text{s.t.} \quad & \mathcal{P}_c(\eta) \geq \epsilon. \end{aligned}$$

Note that the objective function of Problem 1 is $\mathcal{E}(P_t)$, which is presented using (28) and (29). From (9), we can also present the constraint using the AoI violation probability as

$$\begin{aligned} \mathcal{P}_c(\eta) &\geq \epsilon \\ \Leftrightarrow \mathcal{P}_v \left(\frac{u}{v} \sqrt{\frac{S_c(\theta_{\text{th}})}{\pi}} (1 - \sqrt{\eta}) \right) &\leq 1 - \epsilon \end{aligned} \quad (30)$$

where $\mathcal{P}_v(v_{\text{th}})$ is given in (16). Furthermore, P_t can also be presented as a function of p_s , i.e., $P_t = f_s^{-1}(p_s)$, where $f_s(P_t)$ is defined in (2). Since the function $f_s(P_t)$ is bijective, we can make the equivalent problem of Problem 1 as a minimization problem over p_s instead of P_t .

In addition, in Corollary 1, we show that $\mathcal{P}_v(v_{\text{th}})$ is a decreasing function of p_s . If we define the AoI violation probability in (16) as a function of p_s , i.e., $\mathcal{P}_v(p_s)$ for better presentation, the constraint in (30) can be represented as³

$$\mathcal{P}_v(p_s) \leq 1 - \epsilon \Leftrightarrow p_s \geq \mathcal{P}_v^{-1}(1 - \epsilon). \quad (31)$$

Therefore, the average energy consumption minimization problem can be finally represented as

Problem 2 (Equivalent problem to Problem 1):

$$\begin{aligned} \min_{p_s} \quad & \frac{E_s}{N} + \frac{T_0 f_s^{-1}(p_s) \left\{ 1 - (1-p_s)^N \right\}}{N p_s} = \mathcal{E}(p_s) \\ \text{s.t.} \quad & p_s \geq \mathcal{P}_v^{-1}(1 - \epsilon) = p_{\text{cov}}. \end{aligned}$$

Note that $f_s^{-1}(p_s)$ cannot be presented in a closed form for general environments. Hence, we consider two environments

³Unfortunately, it is hard to obtain the exact value of $\mathcal{P}_v^{-1}(1 - \epsilon)$ in a closed-form expression, but it can be readily obtained numerically.

for the optimization: the noise-limited and the interference-limited environments. From (2), we can then present $f_s^{-1}(p_s)$ in a closed form as

$$f_s^{-1}(p_s) = \begin{cases} -\frac{\xi}{\ln p_s}, & \text{noise-limited} \\ \zeta \left(-\frac{1}{\ln p_s}\right)^{\alpha/2}, & \text{interference-limited.} \end{cases} \quad (32)$$

After presenting $f_s^{-1}(p_s)$ as (32) and (33), we can see that the objective function $\mathcal{E}(p_s)$ is not a convex, so it is hard to obtain the optimal solution. However, since the objective function becomes differentiable, we first investigate the stationary points of the objective function, satisfying the constraint as follows.

Proposition 1: Regardless of system parameter values, $\mathcal{E}(p_s)$ has two stationary points for the following range of the maximum retransmission number N :

- $N \geq 9$ in the noise-limited environment
- $N \geq f_1(\alpha)$ in the interference-limited environment

where the values of $f_1(\alpha)$ are provided in Fig. 5 for the pathloss exponent $2 \leq \alpha \leq 4$. In other range of N , $\mathcal{E}(p_s)$ does not have any stationary point.

Proof: In the noise-limited environment, by substituting (32) into (28), $\mathcal{E}(p_s)$ is presented as

$$\mathcal{E}(p_s) = \frac{E_s}{N} - \frac{\xi T_o \left\{1 - (1 - p_s)^N\right\}}{N p_s \ln p_s}. \quad (34)$$

From (34), we obtain the derivative of $\mathcal{E}(p_s)$ with respect to p_s as

$$\frac{d\mathcal{E}(p_s)}{dp_s} = \frac{\xi T_o}{N} f_1(p_s, N) \quad (35)$$

where

$$f_1(p_s, N) = \frac{(1 + \ln p_s) \left\{1 - (1 - p_s)^N\right\} - N p_s (1 - p_s)^{N-1} \ln p_s}{p_s^2 (\ln p_s)^2}. \quad (36)$$

In (35), $\frac{\xi T_o}{N} > 0$ and $f_1(p_s, N)$ is a function of the parameters p_s and N only. Hence, the stationary points that make $\frac{d\mathcal{E}(p_s)}{dp_s} = 0$ are determined by $f_1(p_s, N) = 0$ and they are affected by N only. Nevertheless, for given N , it is difficult to present the exact value of p_s that makes $f_1(p_s, N) = 0$. However, by plotting $f_1(p_s, N)$, we can readily find p_s that makes $f_1(p_s, N) = 0$, which are the stationary points. In Fig. 4, we plot $f_1(p_s, N)$ for different values. In this figure, we can see that if $N \geq 9$, there exist two stationary points, marked by circles, otherwise, there is no stationary point.

In the interference-limited environment, by substituting (33) into (28), we can present $\mathcal{E}(p_s)$ as

$$\mathcal{E}(p_s) = \frac{E_s}{N} + \frac{\zeta T_o \left\{1 - (1 - p_s)^N\right\}}{N p_s (-\ln p_s)^{\alpha/2}}. \quad (37)$$

In (37), we have

$$\frac{d\mathcal{E}(p_s)}{dp_s} = \frac{\zeta T_o}{2N} f_2(p_s, N, \alpha) \quad (38)$$

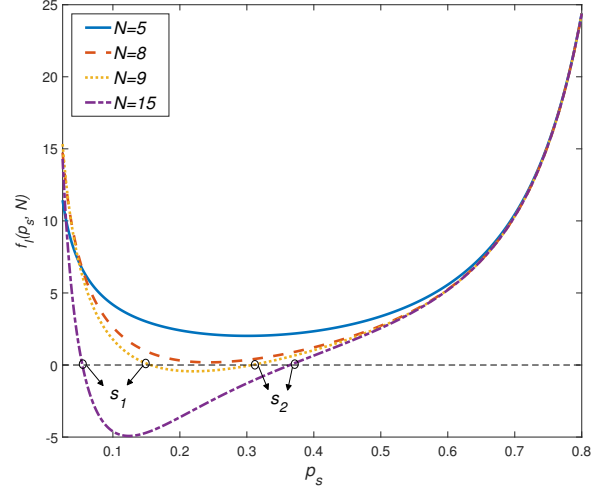


Fig. 4. $f_1(p_s, N)$ in the proof of Proposition 1 as a function of p_s for different values of N

where $f_2(p_s, N, \alpha)$ is given by

$$f_2(p_s, N, \alpha) = \frac{(\alpha + 2 \ln p_s) \left\{1 - (1 - p_s)^N\right\} - 2N p_s (1 - p_s)^{N-1} \ln p_s}{p_s^2 (-\ln p_s)^{\frac{2+\alpha}{2}}}. \quad (39)$$

In (38), $f_2(p_s, N, \alpha)$ is a function of p_s , N and α , so the stationary points are only affected by N and α . Since $\frac{\zeta T_o}{2N} > 0$, p_s which makes $f_2(p_s, N, \alpha) = 0$ becomes the stationary point. Similar to $f_1(p_s, N)$, we can readily know that $f_2(p_s, N, \alpha)$ also gives two stationary points for larger N than a certain value $f_1(\alpha)$, which is differently determined by α . For smaller $N < f_1(\alpha)$, there exists no stationary point. After checking $f_2(p_s, N, \alpha)$ for different α , we obtain the value $f_1(\alpha)$ for $2 \leq \alpha \leq 4$ as Fig. 5. ■

From Proposition 1, we can know that when N is small, $\mathcal{E}(p_s)$ increases with p_s since $\frac{d\mathcal{E}(p_s)}{dp_s} > 0$. This means it cannot be energy-efficient if we use larger transmission power to increase the STP in this case. We can also obtain the optimal value of the STP in the following Lemma.

Lemma 2: For $N \geq 9$ in the noise-limited environment and $N \geq f_1(\alpha)$ in the interference-limited environment, the optimal STP p_s^* that minimizes $\mathcal{E}(p_s)$ is given by

$$p_s^* = \begin{cases} s_2, & \text{if } s_1 < p_{\text{cov}} < s_2, \\ p_{\text{cov}}, & \text{if } s_2 \leq p_{\text{cov}}, \\ \arg \min_{p_s \in \{p_{\text{cov}}, s_2\}} \mathcal{E}(p_s), & \text{if } p_{\text{cov}} \leq s_1 \end{cases} \quad (40)$$

where s_1 and s_2 are two stationary points of $\mathcal{E}(p_s)$, and $s_1 < s_2$, and p_{cov} is given in (31). For $N < 9$ in the noise-limited environment and $N < f_1(\alpha)$ in the interference-limited environment, we have

$$p_s^* = p_{\text{cov}}. \quad (41)$$

Proof: When there exist two stationary points, since $\lim_{p_s \rightarrow 1} \frac{d\mathcal{E}(p_s)}{dp_s} > 0$ in (35) and (38), we can know that s_1 and s_2 are local maximum and minimum, respectively. Since

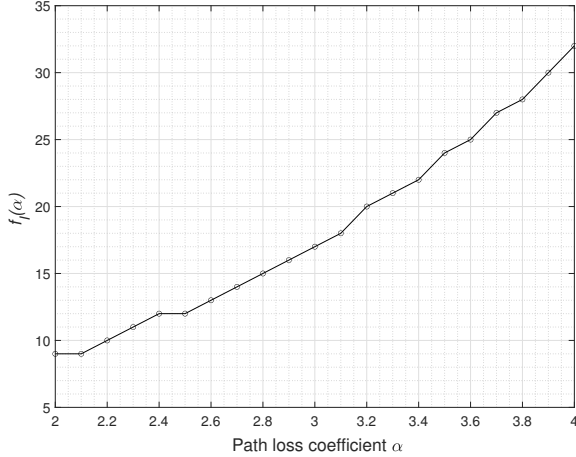


Fig. 5. Minimum value of N which gives two stationary points $f_1(\alpha)$ as a function of path loss coefficient α .

$p_s \geq p_{\text{cov}}$ from the constraint in (31), when $s_1 < p_{\text{cov}} < s_2$, s_2 becomes the optimal p_s . When $p_{\text{cov}} \geq s_2$, since $\mathcal{E}(p_s)$ keeps increasing with p_s , p_{cov} becomes the optimal. On the other hand, when $p_{\text{cov}} \leq s_1$, the optimal STP can be selected between p_{cov} and s_2 as the one providing smaller $\mathcal{E}(p_s)$. Lastly, when there is no stationary point, $\mathcal{E}(p_s)$ is a strictly increasing function of p_s . Therefore, p_{cov} becomes the optimal STP. ■ Once we obtain the optimal STP p_s^* as in Lemma 2, we can also present the optimal transmission power as

$$P_t^* = f_s^{-1}(p_s^*), \quad (42)$$

where $f_s^{-1}(p_s)$ is given in (32) and (33). In addition, from Lemma 2, we can see the effect of N on the optimal transmission power P_t^* as follows.

Corollary 2: The optimal transmission power P_t^* increases as the maximum number of retransmissions N increases.

Proof: As N increases, the AoI violation probability in (31) increases, which makes p_{cov} in (31) larger. We can also see that when there exist two stationary points, the increase of N makes the gap between s_1 and s_2 bigger, as also shown in Fig. 4. From these results, p_s^* in (40) increases with N since both s_2 and p_{cov} increase. On the other hand, when the stationary point does not exist, as can be seen in (41), p_s^* is only determined by p_{cov} which increases as N increases. ■ From Corollary 2, we can see that it is better to use larger transmission power P_t as N increases for lower average energy consumption.

V. NUMERICAL RESULTS

In this section, we present the numerical results of the AoI performance for the sensor monitoring system. We have also verified the analysis results with the Monte-Carlo simulation, which is conducted by MATLAB. Unless otherwise specified, the values of system parameters presented in Table II are used.

Figure 6 presents the average AoI as a function of the transmission power P_t with the different values of the maximum

TABLE II
PARAMETER VALUES IF NOT OTHERWISE SPECIFIED

Parameters	Values	Parameters	Values
λ_1, λ_2 [nodes/m ²]	8.7×10^{-5}	α	3.5
P_1 [mW]	40	P_2 [mW]	30
d [m]	20	δ	1
T_R	1	T_o	1
θ_{th}	0.1	η	0.6
ϵ	0.6	N_o	10^{-5}
E_s [mW]	1		

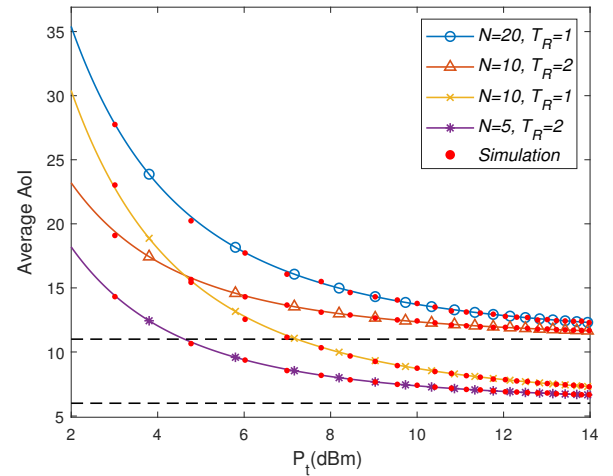


Fig. 6. Average AoI as a function of transmission power P_t for different values of N and T_R .

number of transmissions N and the transmission interval T_R . From Fig. 6, we can see that the analysis results fit well with the simulation results. Obviously, the average AoI decreases as P_t increases. This is because the peak AoI of each update decreases due to the less retransmissions. We can also see that the average AoI increases as N increases because of the longer sensing period NT_R . Furthermore, we can see that the average AoIs of two cases with $NT_R = 10$ and $NT_R = 20$ converge to the same value (i.e., 6 and 11, respectively) because large P_t make the communication successful without retransmission and the updates can occur every sensing period NT_R .

Figure 7 shows the AoI violation probability as a function of transmission power P_t for different values of N with $v_{\text{th}} = 10$. As discussed in Corollary 1, the AoI violation probability decreases as P_t increases due to the smaller number of retransmissions. We can see that the AoI violation probability increases as N increases because of the longer sensing period NT_R . We can also see that as the main link distance increases, the AoI violation probability increases because of low STP.

Figure 8 presents the average energy consumption as a function of P_t for different values of N in the noise-limited environment. Here, we use $u = 1.76 \times 10^{-2}$, $v = 1.2 \times 10^{-3}$, and $r_{\text{max}} = 3$. Each graph is plotted for a feasible transmission power which satisfies the coverage constraint (31). As can be

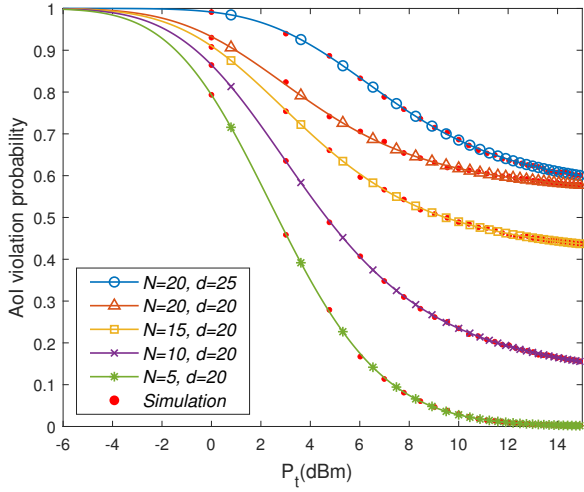


Fig. 7. AoI violation probability $\mathcal{P}_v(v_{th})$ as a function of the transmission power P_t with $v_{th} = 10$ for different values of N .

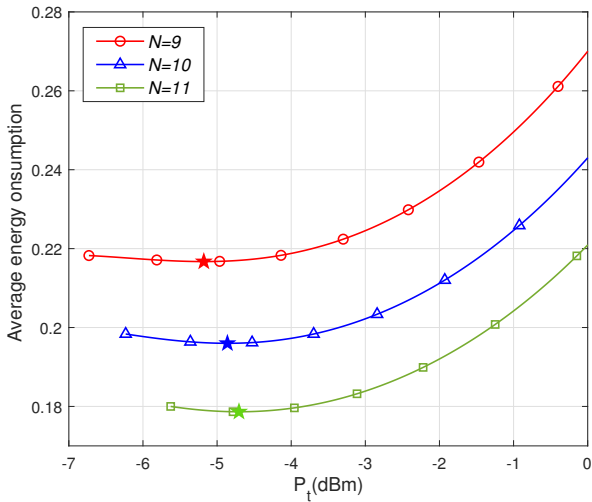


Fig. 8. Average energy consumption as a function of transmission power P_t with $T_R = 1$ for different values of N in noise-limited environment.

seen in Fig. 8, $\mathcal{E}(P_t)$ decreases and then increases. This is because, for small P_t , as P_t increases, the reduced number of retransmissions (which lowers $\mathcal{E}(P_t)$) more dominantly affect than the increased P_t (which enlarges $\mathcal{E}(P_t)$). However, when P_t is larger than a certain value, the retransmission number is not reduced anymore as the STP is almost one, so increasing P_t increases $\mathcal{E}(P_t)$. Therefore, there exist the optimal transmission power P_t^* that minimizes the average energy consumption such as $P_t^* = -5.18$ dBm for $N = 9$, which is consistent with the first case result of Lemma 2. Moreover, as discussed in Corollary 2, we can see that the optimal transmission power P_t^* increases with the maximum number of transmissions N , which indicates that the sensor needs to use larger transmission power when the sampling period becomes longer.

Figure 9 presents the average energy consumption as a function of P_t for different N with and without the interference-limited environment assumption. For both cases, we use $u =$

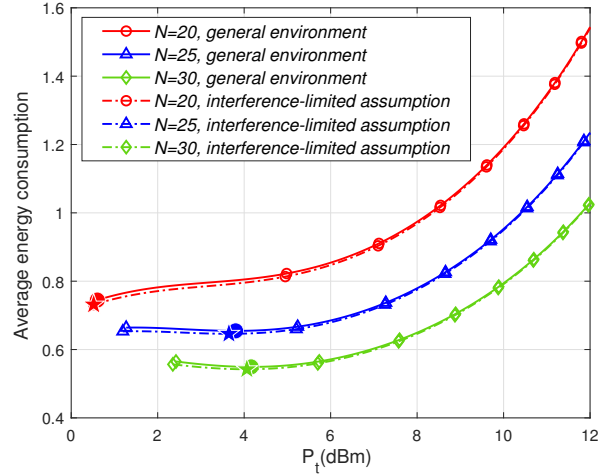


Fig. 9. Average energy consumption as a function of the transmission power P_t for different values of N for general environment and with interference-limited assumption when $N_0 = 10^{-6}$.

1.76×10^{-2} , $v = 4.4 \times 10^{-4}$, and $r_{max} = 3$. In Fig. 9, circle symbols represent the optimal transmission power P_t^* that minimizes the average energy consumption in general environment, and star symbols represent P_t^* with the interference-limited assumption. Since the STP is lower in the general environment than that with the interference-limited assumption for the same P_t , the average energy consumption in the general environment is higher than that with the interference-limited assumption. Similar to the results in the noise-limited environment, we can see that P_t^* is higher for larger N . Since the STP is higher in the case with the interference-limited assumption than the general environment as the noise power is ignored, we can observe that P_t^* as well as the average energy consumption are higher in the general environment than those with the interference-limited assumption. Therefore, P_t^* with the interference-limited assumption can provide the lower bound of the real optimal transmission power, but the results with the interference-limited assumption become more valid and similar to the real optimal value as the effect of the interference increases (i.e., as λ_I increases).

Figure 10 shows the average energy consumption as functions of P_t and N in the noise-limited environment. The graph is plotted for the feasible range of P_t , which satisfies the coverage constraint in (31). In addition, the circle symbols in Fig. 10 refer to the optimal transmission power P_t^* which minimizes the average energy consumption for each N . From Fig. 10, we can see that the minimum transmission power P_{cov} which satisfies the coverage constraint increases as N increases. It is because p_{cov} that satisfies the target violation threshold in (31) increases as the AoI violation probability increases for each p_s as N increases. We can also see that when $N \geq 9$, there exist the stationary points as discussed in Proposition 1, so P_t^* becomes higher than P_{cov} . As also shown in Corollary 2, we can also observe that P_t^* increases as N increases.

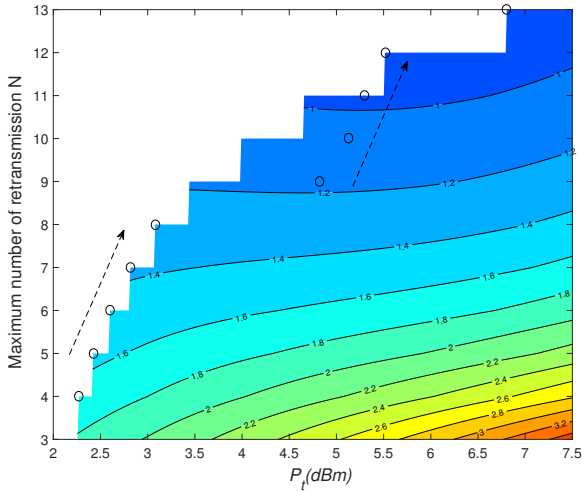


Fig. 10. Average energy consumption as functions of the transmission power P_t and the maximum number of transmissions N with $T_R = 1$ in noise-limited case. The optimal transmission powers that minimize the average energy consumption are marked by circles.

VI. CONCLUSION

In this paper, we consider the sensor monitoring system, which requires maintaining fresh data at the DC. After defining the ETS coverage by reflecting the spatial-temporal correlation of the sensing information, we derive the average AoI and the AoI violation probability. We then finally provide the η -coverage probability, and analytically show it increases with the transmission power of the sensor. We also provide the optimal transmission power of the sensor that minimizes the average energy consumption of the sensor. Our results provide some insights on the energy-efficient design of the sensor monitoring system that requires securing fresh data. Specifically, when the maximum number of retransmissions is small, the minimum power that satisfies the constraint of the η -coverage probability becomes the optimal. The optimal transmission power also increases with the maximum number of retransmissions. This work paves the way to efficient design of the AoI-sensitive sensor networks.

APPENDIX

A. Proof of Theorem 1

We first analyze the violated time g_k , which is defined as

$$g_k = \begin{cases} 0, & \text{if } v_{\text{th}} > NT_R + X_k, \\ NT_R + X_k - v_{\text{th}}, & \text{if } Z_{k-1} \leq v_{\text{th}} \leq NT_R + X_k, \\ Y_{k-1} + X_k, & \text{if } v_{\text{th}} < Z_{k-1}, \end{cases} \quad (43)$$

where $NT_R + X_k$ represents the k th peak of AoI. Note that $Z_{k-1} \leq NT_R, \forall k$. From (43), by using the independence of Z_{k-1} and X_k ⁴, the expectation of g_k is given by

$$\mathbb{E}[g_k] = \mathcal{P}_{g,1} \mathbb{P}[Z_{k-1} \leq v_{\text{th}}] \mathbb{P}[NT_R + X_k > v_{\text{th}}] + \mathcal{P}_{g,2} \mathbb{P}[Z_{k-1} > v_{\text{th}}] \quad (44)$$

⁴Note that X_k is a dependent variable on Z_k . However, since Z_{k-1} and Z_k are independent, X_k and Z_{k-1} are independent as well.

where $\mathcal{P}_{g,1}$ and $\mathcal{P}_{g,2}$ are

$$\begin{aligned} \mathcal{P}_{g,1} &= \mathbb{E}[NT_R + X_k - v_{\text{th}} | Z_{k-1} \leq v_{\text{th}}, NT_R + X_k > v_{\text{th}}] \\ \mathcal{P}_{g,2} &= \mathbb{E}[Y_{k-1} + X_k | Z_{k-1} > v_{\text{th}}]. \end{aligned} \quad (45)$$

Here, $\mathbb{E}[g_k]$ needs to be analyzed differently for the cases of $v_{\text{th}} \leq NT_R$ and $v_{\text{th}} > NT_R$ as follows.

1) *Case 1* ($v_{\text{th}} \leq NT_R$): For $v_{\text{th}} \leq NT_R$, we have

$$\mathbb{P}[Z_{k-1} \leq v_{\text{th}}] = \sum_{n=1}^{\chi} \frac{(1-p_s)^{n-1} p_s}{1-(1-p_s)^N} = \frac{1-(1-p_s)^\chi}{1-(1-p_s)^N}, \quad (46)$$

$$\mathbb{P}[Z_{k-1} > v_{\text{th}}] = 1 - \mathbb{P}[Z_{k-1} \leq v_{\text{th}}] = \frac{(1-p_s)^\chi - (1-p_s)^N}{1-(1-p_s)^N}, \quad (47)$$

$$\mathbb{P}[NT_R + X_k > v_{\text{th}}] = 1, \quad (48)$$

where χ is the maximum number of transmissions, allowed within v_{th} , given by

$$\chi = \left\lfloor \frac{v_{\text{th}} - T_o}{T_R} \right\rfloor + 1. \quad (49)$$

Similar to (19), $\mathcal{P}_{g,1}$ can be obtained as

$$\mathcal{P}_{g,1} = NT_R - v_{\text{th}} + \left(\frac{1}{p_s} - 1 \right) T_R + T_o. \quad (50)$$

In (45), $\mathcal{P}_{g,2}$ can also be obtained as

$$\begin{aligned} \mathcal{P}_{g,2} &= \mathbb{E}[NT_R - Z_{k-1} + X_k | Z_{k-1} > v_{\text{th}}] \\ &= NT_R + \frac{T_R}{p_s} - \sum_{n=\chi+1}^N \frac{p_s T_R n (1-p_s)^{n-1}}{(1-p_s)^\chi - (1-p_s)^N} \\ &= NT_R + \frac{T_R}{p_s} \\ &\quad - \frac{T_R \left\{ (1-p_s)^\chi (1+p_s \chi) - (1-p_s)^N (1+p_s N) \right\}}{p_s \left\{ (1-p_s)^\chi - (1-p_s)^N \right\}}. \end{aligned} \quad (51)$$

By substituting (46)–(51) into (44), we can express $\mathbb{E}[g_k]$ as

$$\begin{aligned} \mathbb{E}[g_k] &= \frac{\{p_s (T_o - T_R - v_{\text{th}}) + T_R\} \{1 - (1-p_s)^\chi\}}{p_s \{1 - (1-p_s)^N\}} \\ &\quad + \frac{T_R \{N - \chi(1-p_s)^\chi\}}{1 - (1-p_s)^N}. \end{aligned} \quad (52)$$

Finally, by dividing (52) by (24) and replacing χ with (49), $\mathcal{P}_v(v_{\text{th}})$ for the case of $v_{\text{th}} \leq NT_R$ is presented as the first equation in (16).

2) *Case 2* ($v_{\text{th}} > NT_R$): In (44), we have

$$\mathbb{P}[Z_{k-1} \leq v_{\text{th}}] \stackrel{(a)}{=} 1, \quad \mathbb{P}[Z_{k-1} > v_{\text{th}}] \stackrel{(a)}{=} 0 \quad (53)$$

$$\begin{aligned} \mathbb{P}[NT_R + X_k > v_{\text{th}}] &= \sum_{n=\chi-N+1}^{\infty} (1-p_s)^{n-1} p_s \\ &= (1-p_s)^{\chi-N}, \end{aligned} \quad (54)$$

where (a) is obtained by the fact $Z_{k-1} \leq NT_R$. We also obtain $\mathcal{P}_{g,1}$ as

$$\mathcal{P}_{g,1} = T_R \left(\frac{1}{p_s} + \chi - 1 \right) + T_o - v_{\text{th}}. \quad (55)$$

Here, $\mathcal{P}_{g,2}$ is not presented since $\mathbb{P}[Z_{k-1} > v_{\text{th}}] = 0$ in (44). By substituting (53)–(55) into (44), we finally obtain $\mathbb{E}[g_k]$ for the case of $v_{\text{th}} > NT_{\text{R}}$ as

$$\mathbb{E}[g_k] = \left\{ T_{\text{R}} \left(\frac{1}{p_{\text{s}}} + \chi - 1 \right) + T_{\text{o}} - v_{\text{th}} \right\} \times (1 - p_{\text{s}})^{\chi - N}. \quad (56)$$

By dividing (56) by (24) and replacing χ with (49), we obtain $\mathcal{P}_{\text{v}}(v_{\text{th}})$ as the second equation in (16).

REFERENCES

- [1] J. Kim, M. Kim, and J. Lee, “Sensing and transmission design for aoi-sensitive wireless sensor networks,” in *Proc. IEEE Global Commun. Conf. (GlobeCom) Workshop*, Taipei, Taiwan, Dec. 2020, pp. 1–6.
- [2] M. E. Yazid Boudaren, M. R. Senouci, M. A. Senouci, and A. Mellouk, “New trends in sensor coverage modeling and related techniques: A brief synthesis,” in *2014 International Conference on Smart Communications in Network Technologies (SaCoNeT)*, 2014, pp. 1–6.
- [3] R. Elhabyan, W. Shi, and M. St-Hilaire, “Coverage protocols for wireless sensor networks: Review and future directions,” *Int. J. of Commun. Networks*, vol. 21, no. 1, pp. 45–60, 2019.
- [4] B. Wang, J. Zhu, L. T. Yang, and Y. Mo, “Sensor density for confident information coverage in randomly deployed sensor networks,” *IEEE Trans. Wireless Commun.*, vol. 15, no. 5, pp. 3238–3250, 2016.
- [5] F. Yuan, Y. Zhan, and Y. Wang, “Data density correlation degree clustering method for data aggregation in WSN,” *IEEE Sensors J.*, vol. 14, no. 4, pp. 1089–1098, 2014.
- [6] M. K. Abdel-Aziz, S. Samarakoon, C. Liu, M. Bennis, and W. Saad, “Optimized age of information tail for ultra-reliable low-latency communications in vehicular networks,” *IEEE Transactions on Communications*, vol. 68, no. 3, pp. 1911–1924, 2020.
- [7] S. Kaul, R. Yates, and M. Gruteser, “Real-time status: How often should one update?” in *Proc. IEEE Conf. on Computer Commun.*, Orlando, FL, USA, Mar. 2012, pp. 2731–2735.
- [8] M. Moltafet, M. Leinonen, and M. Codreanu, “Closed-form expression for the average age of information in a multi-source M/G/1 queueing model,” in *Proc. IEEE Inf. Theory Workshop*, Visby, Sweden, Aug. 2019, pp. 1–5.
- [9] A. M. Bedewy, Y. Sun, and N. B. Shroff, “Minimizing the age of information through queues,” *IEEE Trans. Inf. Theory*, vol. 65, no. 8, pp. 5215–5232, 2019.
- [10] M. Costa, M. Codreanu, and A. Ephremides, “On the age of information in status update systems with packet management,” *IEEE Trans. Inf. Theory*, vol. 62, no. 4, pp. 1897–1910, 2016.
- [11] R. Devassy, G. Durisi, G. C. Ferrante, O. Simeone, and E. Uysal-Biyikoglu, “Delay and peak-age violation probability in short-packet transmissions,” in *Proc. IEEE Int. Symp. on Inf. Theory*, Vail, CO, USA, Jun. 2018, pp. 2471–2475.
- [12] J. Seo and J. Choi, “On the outage probability of peak age-of-information for D/G/1 queueing systems,” *IEEE Commun. Lett.*, vol. 23, no. 6, pp. 1021–1024, 2019.
- [13] A. Kosta, N. Pappas, A. Ephremides, and V. Angelakis, “The cost of delay in status updates and their value: Non-linear ageing,” *IEEE Trans. Commun.*, vol. 68, no. 8, pp. 4905–4918, 2020.
- [14] Y. Sun and B. Cyr, “Sampling for data freshness optimization: Non-linear age functions,” *Int. J. of Commun. Networks*, vol. 21, no. 3, pp. 204–219, 2019.
- [15] H. Tang, J. Wang, Z. Tang, and J. Song, “Scheduling to minimize age of synchronization in wireless broadcast networks with random updates,” *IEEE Trans. Wireless Commun.*, vol. 19, no. 6, pp. 4023–4037, 2020.
- [16] D. Li, S. Wu, Y. Wang, J. Jiao, and Q. Zhang, “Age-optimal harq design for freshness-critical satellite-iot systems,” *IEEE Internet of Things Journal*, vol. 7, no. 3, pp. 2066–2076, 2020.
- [17] B. Yu, Y. Cai, D. Wu, and Z. Xiang, “Average age of information in short packet based machine type communication,” *IEEE Transactions on Vehicular Technology*, vol. 69, no. 9, pp. 10306–10319, 2020.
- [18] Y. Gu, H. Chen, Y. Zhou, Y. Li, and B. Vucetic, “Timely status update in internet of things monitoring systems: An age-energy tradeoff,” *IEEE Internet Things J.*, vol. 6, no. 3, pp. 5324–5335, Jun. 2019.
- [19] J. Gong, X. Chen, and X. Ma, “Energy-age tradeoff in status update communication systems with retransmission,” in *Proc. IEEE Global Telecomm. Conf.*, Abu Dhabi, United Arab Emirates, Dec. 2018, pp. 1–6.
- [20] S. Poojary, S. Bhambay, and P. Parag, “Real-time status updates for correlated source,” in *Proc. IEEE Inf. Theory Workshop*, Kaohsiung, Taiwan, Nov. 2017, pp. 274–278.
- [21] J. Hribar, M. Costa, N. Kaminski, and L. A. DaSilva, “Using correlated information to extend device lifetime,” *IEEE Internet Things J.*, vol. 6, no. 2, pp. 2439–2448, Apr. 2019.
- [22] Y. Sun and B. Cyr, “Information aging through queues: A mutual information perspective,” in *Proc. IEEE Workshop on Signal Process. Advances in Wireless Commun.*, Kalamata, Greece, Jun. 2018, pp. 1–5.
- [23] J. Lee, J. G. Andrews, and D. Hong, “Spectrum-sharing transmission capacity with interference cancellation,” *IEEE Trans. Commun.*, vol. 61, no. 1, pp. 76–86, 2013.
- [24] I. S. Gradshteyn and I. M. Ryzhik, *Table of integrals, series, and products*, 7th ed. Elsevier/Academic Press, 2007.
- [25] J. P. Champati, H. Al-Zubaidy, and J. Gross, “On the distribution of AoI for the GI/GI/1/1 and GI/GI/1/2* systems: Exact expressions and bounds,” in *Proc. IEEE Conf. on Computer Commun.*, Paris, France, Apr. 2019, pp. 37–45.